2012 International Conference on Image, Vision and Computing (ICIVC 2012)
IPCSIT vol. 50 (2012) © (2012) IACSIT Press, Singapore
DOI: 10.7763/IPCSIT.2012.V50.15

Imaging with Hexagonal Segmented Mirror in the Presence of Kolmogorov Atmospheric Turbulence

A. T. Mohammed [+] and A. J. Tawfiq

Dept. of Astronomy, College of Science, University of Baghdad

Abstract. Two-dimensional computer simulations are carried out to investigate the quality of observing astronomical objects with hexagonal segmented mirror in the presence of Kolmogorov turbulence. In the absence of atmospheric turbulence, the height of the central spike that appears in the modulation transfer function of a reference star is directly proportional to the number of hexagons. In the presence of atmospheric turbulence, the number of hexagons has little effect on the height of the point spread function and the average frequency components of the modulation transfer function when the area of each hexagon is less than 0.05 times the area of a unit circle (area of the aperture that to be filled with hexagons). The number of hexagons has not significantly change the height of the secondary peaks of the autocorrelation function of a binary star even at very good seeing condition.

Keywords: image formation**,** fourier transform, telescope segmented mirror.

1. Introduction

The hexagonal aperture is a modification of a circular aperture. It is desirable for multiple mirror system. Primary mirrors of the next generation of extremely large optical telescope will be highly segmented and equipped with adaptive optics(AO). Although upcoming telescopes use hexagonal apertures, the diffraction effects from such segmentation is not widely treated in the literature (for more details, see [1-4]).

The nature of the wave front perturbations introduced by atmospheric turbulence are presented by the Kolmogorov model that developed by Tatarski [5]. This model is supported by many experimental research and is widely used in simulations of imaging through atmospheric turbulence [6-17]. This model assigns the perturbation in the wave front due to the variations in the refractive index of the atmosphere. This variation leads directly to phase fluctuations. The amplitude fluctuations are considered to be of a secondary order effect.

There are very few publications in the literatures that considered imaging with giant segmented mirror ground based optical telescope in the presence of atmospheric turbulence, for mor details see[18-20]. It is for that reason we have developed an analytical model and its quality assessments that describe imaging of astronomical objects with hexagonal segmented mirror.

2. Theoretical Formulations

Assume a plane wave of unit amplitude be incidant on a segmented aperture. The electric field could be defined as the sum of the electric fields over all N segments in the aperture.

$$E(x,y)=\sum_{n=1}^{N}E_n(\vec{x}-\vec{r}_n,\vec{y}-\vec{r}_n) \tag{1}$$

where E_n is the complex field that resulted from the segment centred at (r_n,r_n), the n^{th} position.

[+] Corresponding author. Tel.: + 07702917735.
E-mail address: ali.talib@scbaghdad.edu.iq.

If we define a segment's shape function as *As(x,y)* which equals unity inside the segment and zero outside, then each segments phase error is independent. The field distribution from the n th segment is given by:

$$E(\vec{x}-r_n, y-\vec{r}_n) = As(\vec{x}-\vec{r}_n, \vec{y}-\vec{r}_n)\exp\left[j\phi_n(\vec{x}-\vec{r}_n, \vec{y}-\vec{r}_n\right] \tag{2}$$

In the presence of atmospheric turbulence $E(\vec{x},\vec{y})$ could be described as the complex wavefront from a star, *U(x,y)*. The global optical transfer function,OTF of an incoherent system is given by [21]:

$$T(u,v) = \frac{\int\int_{-\infty}^{+\infty} A(x,y)A^*(x-\lambda fu, y-\lambda fv)U(x,y)U^*(x-\lambda fu, y-\lambda fv)dxdy}{\int\int_{-\infty}^{+\infty} |A(x,y)|^2 |U(x,y)|^2 dxdy} \tag{3}$$

where A and A* are the complex pupil function and its complex conjugate, U and U* are the perturbed complex wave front and its complex conjugate that introduce by atmospheric turbulence , f is the focal length of the lens, λ is a wavelength, and u, v are spatial frequency variables. The modulation transfer function, (*MTF*) is taken to be $|T(u,v)|$. Equation (3) represents the summation of OTF over N segments.

The point spread function (psf) could be defined as the absolute of the inverse Fourier transform of equation (3). psf is always nonnegative and real.

The probability density function of the complex amplitude of the perturbed wave front from the star, $U(x, y)$, is considered to obey Kolmogorov statistics. We have to assume there is a phase screen in the aperture of the optical telescope. The Kolmogorov power spectral density, PSD , is given by [22]:

$$PSD(k) = 0.023\ r_o^{-5/3}|k|^{-11/3} \tag{4}$$

where r_o is the Fried parameter [23].

3. Computational Methods

Two-dimensional computer simulations are carried out to investigate the quality of images that recorded by an optical telescope in the presence of Kolmogorov atmospheric turbulence. The strength of atmospheric turbulence (sc) is strongly related to r_o and the radius of the optical telescope (R),

$$sc = r_o / R, \qquad 0 < sc \le 1$$

The following steps are considered in generating a perturbed wave front of a reference star:

a-The perturbed complex wave front of a reference star, *U(x, y)*, that introduced by atmospheric turbulence is generated by assigning a normal random distribution with zero mean and unit variance to its real and imaginary parts using different realizations.

b- *PSD* is computed according to equation (4) using

$$k = \left[\left(i-N_C\right)^2 + \left(j-N_C\right)^2\right]^{1/2} \tag{5}$$

Where *(N_C, N_C)* is the central point of a two dimensional array and *(i, j)* are the indices of a point inside an array.

c- Set the central value of *PSD* to zero *(i.e. PSD (N_C, N_C)* = 0). This is equivalent to set piston to zero.

d- Multiply the result of step **a** by the square root of *PSD.*

e- Apply Fourier transform and the real part represents the Kolmogorov phase screen, $\phi(x, y)$.

Finally, the perturbed complex wave front takes the form,

$$U(x,y) = e^{-j\left(\frac{2\pi}{\lambda}\varphi(x,y)\right)} \tag{6}$$

Now, it is so important to extend our study to include a binary star. Each star is taken to be an impulse reference star (one pixel extent and of unity magnitude) as shown below:

$$\delta(n) = \begin{cases} 1 & n = 0 \\ 0 & elsewhere \end{cases} \tag{7}$$

The binary star is a two impulse stars separated by a certain distance from the center of an array. The separation is chosen with respect to the ratio "*separation/D*" ($D = 2R$). This ratio is taken to be 0.1. This will produce a binary star that has a separation to be just within the full extent of the base of the psf of the optical telescope in use (no turbulence). This binary star is then convolved with the psf of the telescope/atmosphere system. The power spectrum and the autocorrelation function at different values of r_0 are then computed. It should be pointed out here that the size of each array is taken to be 256 by 256 pixels. The only exception is the size of the autocorrelation function. In this case, the power spectrum of a binary star of size 256 by 256 is inserted into an array of size 512 by 512 padded with zeros. This is to make sure that the frequency components of the autocorrelation function are vanishing to zero inside this array.

4. Results and Discussions

Figure (1) demonstrates the image of the phase screen function and its surface plot. The mirror is segmented into different number of hexagons (N_h) as displayed in Fig.(2). In the absence of turbulence, the MTF corresponding to Fig.(2) are shown in Fig.(3).

In the presence of kolmogorov turbulence, the psf and MTF of a reference star and the power spectrum and the autocorrelation function of a binary star for different values of r_o and N_h are computed and some selected results are displayed in Figs.(4 to 6). To examine the quality of the results, the following criteria are used to assess psf and MTF :

$$I_{\max} = \max\left[psf(x,y)\right], \quad AF = \sum_{u=1}^{M}\sum_{v=1}^{N}\frac{MTF(u,v)}{MTF(0,0)} \tag{8}$$

where $MTF(0,0)$ is the maximum value of MTF and it is located in the middle of an array.

The quality of the autocorrelation function of a binary star is taking to be the height of its secondary peak (h_a). The physical behavior of $I_{\max}$, AF, and h_a are shown in Fig.(7).

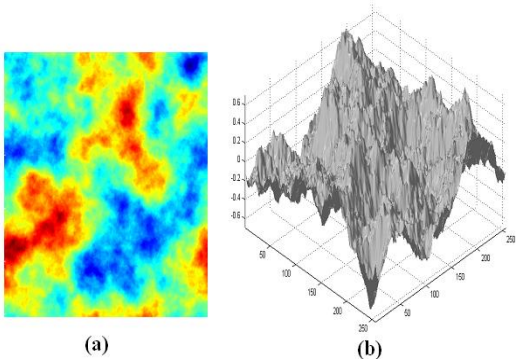

Fig.1: Phase screen function by sampling Kolmogorov spectrum and its surface plot (r_o =1).

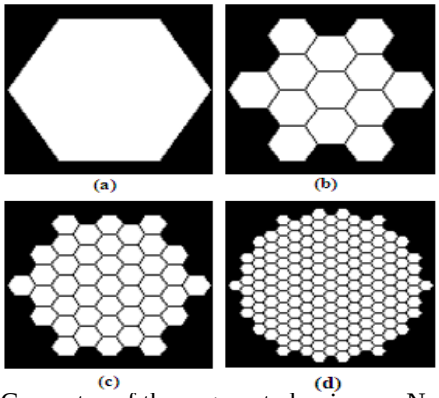

Fig.2: Geometry of the segmented mirror **a-**N_h= 1.**b-** N_h= 13. **c-** N_h= 43. **d-** N_h= 169.

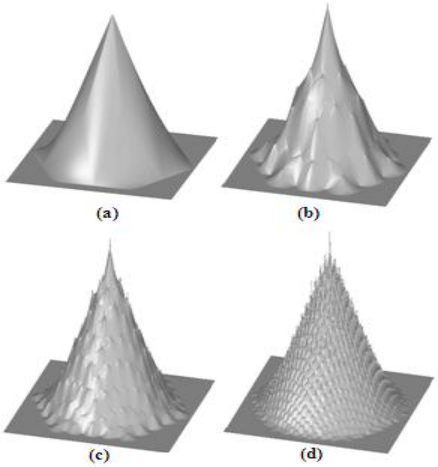

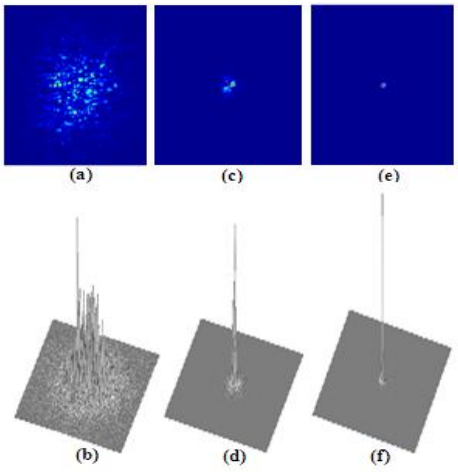

Fig.3: surface plot of MTFs corresponding to Fig. (2): a- Nh= 1. b- Nh=13. c- Nh=43. d-Nh=169.

Fig.4: Nh=1, a,b- psf and its surface plot (r_o =1), c, d- Psf and its surface plot (r_o =5). e,f- psf and its surface plot (r_o =30)

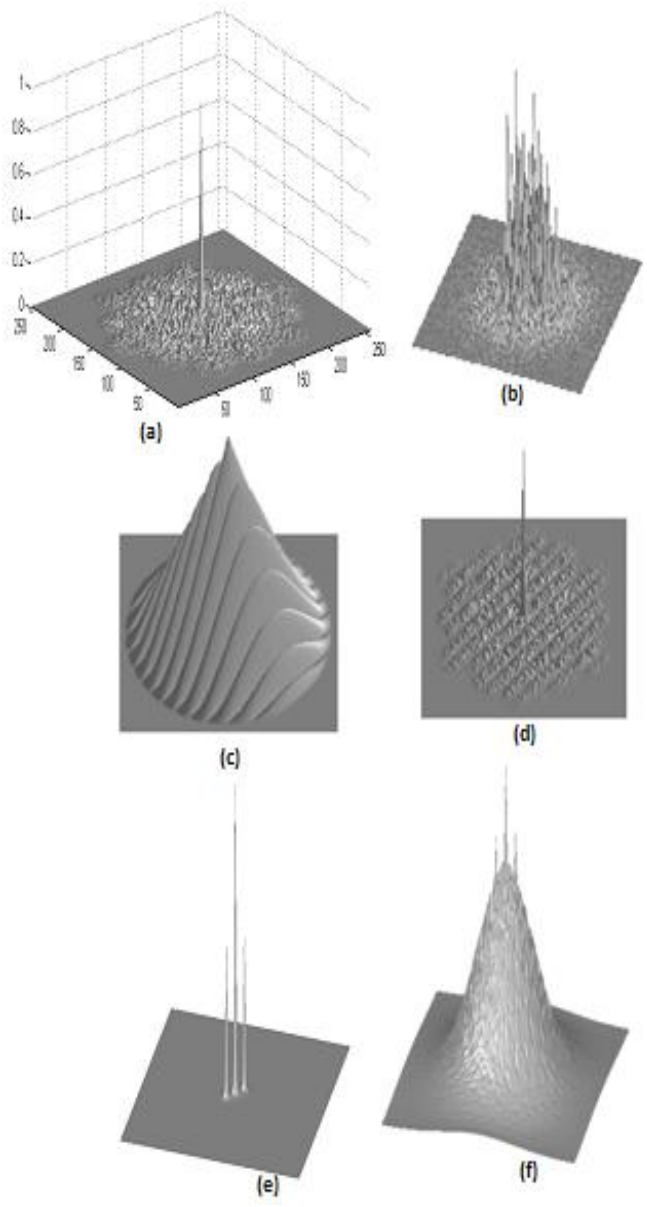

Fig. 5: N_h=1: **a-** Surface plot of MTF (r_o =1). **b-** Binary star (r_o =1).**c**-Typical power spectrum of a binary star (no turbulence). **d**-Power spectrum of (b). **e-** Typical autocorrelation function of a binary star (no turbulence). **f-** Autocorrelation function of (b).

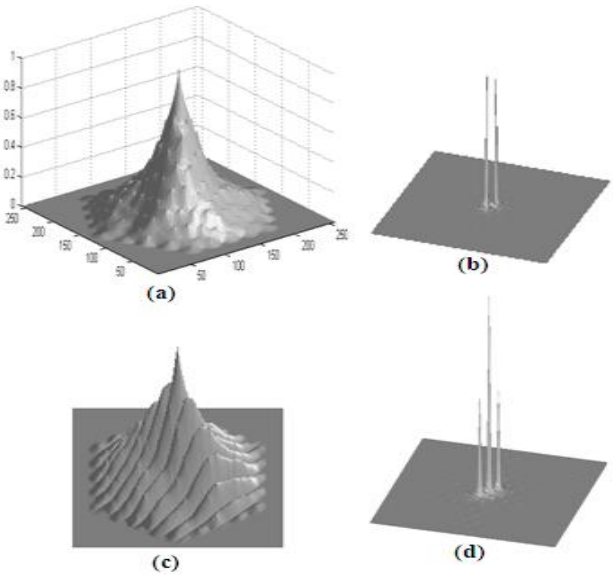

Fig. 6: N_h=43
a-Surf ace plot of MTF (r_o =20). **b-** Binary star (r_o =20). **c-** Power spectrum of (b). **d-** Autocorrelation function of (b).

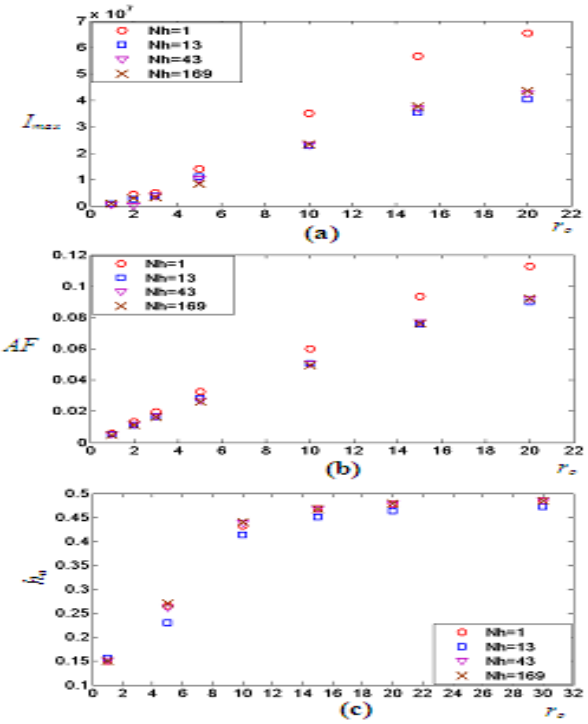

Fig. 7: **a-**The height of psf versus r_o. **b-**Average MTF versus r_o. **c-** h_a versus r_o.

5. Conclusions

In this paper, we have demonstrated the analytical model of imaging with segmented mirror in the presence of Kolmogorov atmospheric turbulence. In the absence of atmospheric turbulence, the number of

hexagons, N_h, has great effect on the structure of psf and MTF. As N_h increases, the little spikes that appear on the surface of MTF become sharper and the height of the central spike increases (see Fig.3). This is attributed to the total area of the gap between hexagons.

In the presence of atmospheric turbulence, N_h has little effects on $I_{\max}$ and AF when the area of each hexagon is less than 0.05 times the area of the aperture even at very good seeing conditions . N_h has not significantly change the height of the secondary peaks of the autocorrelation function of a binary star (h_a) .

6. References

[1] M. Troy, G. Chanan. Diffraction Effects from Giant Segmented Mirror Telescopes. Applied Optics, 2003, **42**:3745-3753.

[2] N. Yaitskova, K. Dohlen, P. Dierickx. Diffraction in OWL: Effects of Segmentation and Segments Edge Misfigure. Proceedings SPIE, 2003, **4840**: 171-182.

[3] N. Yaitskova, K. Dohlen, P. Dierickx. Analytical study of diffraction effects in extremely large segmented telescopes. JOSA A, 2003, **20**: 1563-1575.

[4]G. A. Chanan, M. Troy. Strehl ratio and modulation transfer function of segmented mirror telescopes as functions of segment phase error. Applied Optics, 1999, **38**: 6642-6647.

[5] V. I. Tatarski. Wave propagation in a turbulent medium. 1961. McGraw-Hill, New York.

[6] D. F. Buscher, J. T. Armstrong, C. A. Hummel, A. Quirrenbach, D. Mozukewich, K. J. Johnston, C. S. Denston, M. M. Colarita, and M. Shao,. Interferometric seeing measurements on Mt. Wilson: Power spectra and outer scales. Applied Optics, 1995, **34**(6): 1081-1096.

[7] N. S. Nightingale, and D.F. Buscher. Interferometric seeing measurements at the La Palma observatory. Monthly Notices of the Royal Astronomical society. 1991, **251**: 155-166.

[8] J. W. O'Byrne. Seeing measurements using a shearing interferometer. Publications of the Astronomical Society of the pacific. 1988, **100**: 1169-1177.

[9] M. M. Colavita, M. Sahao, and D. H Staelin. Atmospheric phase measurements with the Mark III stellar interferometer. Applied Optics. 1987, **26**(19): 4106-4112.

[10] R. G. Lane, A. Glindemann, and J.C. Dainty. Simulation of a Kolmogorov phase screen, Waves in Random media.

1992, **2** : 209-224.

[11] T. W. Nicholls, G. D. Boreman, and J. C. Dainty. Use of a shack-Harfmann wavefront sensor to measure deviations from a Kolmogorov phase screen. Optics Letters. 1995, **20**(24): 2460-2462.

[12] R. N. Tubbs. Lucky exposure: Diffraction Limited astronomical imaging through the atmosphere. 2003, PhD thesis, Cambridge University.

[13] H. F. Hormuth, D. J. Butler, W. Brandrer, and H. Thomas. Atmosphere-Like Turbulence Generation with Surface-Etched Phase- Screens. Optics Express. 2006, **14**(22).

[14] N. K. Vereshaging, and P. M. B. Vitanyi. Kolmogrov's structure functions and model selection. IEEE Transaction Teory. 2004, **50**(12).

[15] C. O. F. Jime'nez. Understanding the atmospheric turbulence structure parameter, C_n, in the littoral regime. 2006, A thesis submitted for the degree of master of science in physics university of Puerto Rico Mayaguez Campus.

[16] J. Osborn. Profiling the turbulent atmosphere and novel correction techniques for imaging and photometry in astronomy. 2010, PhD thesis, Department of physics, Durham University.

[17] Liesl, Burger, Igor, A. Litvin, and Andrew Forbes. Simulation atmospheric turbulence using phase-only spatial modulator. South African Journal of Science. 2008, **104**: 129-134.

[18] G. Angeli, A. Segurson, R. Upton, B. Gregory, and M. Cho. International modeling tools for large ground based optical telescopes. Proceedings of the SPIE. 2003, **5178**: 49-63.

[19] G. Angeli, and B. Gregory. Linear optical model for a large ground based telescope. Procedings of the SPIE. 2003, **5178**: 64-73.

[20] J. P. et al. The optical modeling tools for the Canadian very large optical telescope integrated model. Proceeding of the SPIE 2nd Backaskog workshop on extremely large telescopes.2003.

[21] J. W. Goodman. Statistical optics. 2000, a Wiley- Interscience publication.

[22] R. G. Lane, A. Glindemann, and J. C. Dainty. Simulation of a Kolmogorov phase screen. Waves in random media. 1992, **2**: 209-224.

[23] D. L. Fried. Statistics of a geometric representation of wave front distribution. J. Opt. Soc. Am.1965, **55**: 1427-1435.